PRAMANA
— journal of
physics

Vol. 69, No. 3
September 2007
pp. 395–409

Optical parametric amplification beyond the slowly varying amplitude approximation

M HOSSEINI FARZAD
Physics Department, Shiraz University, Shiraz 71454, Iran
E-mail: farzad@susc.ac.ir

MS received 12 November 2006; revised 2 July 2007; accepted 5 July 2007

Abstract. The coupled-wave equations describing optical parametric amplification (OPA) are usually solved in the slowly varying amplitude (SVA) approximation regime, in which the second-order derivatives of the signal and idler amplitudes are ignored and in fact the electromagnetic effects due to exit face of the medium is not involved. Here, an analytical plane-wave solution of these coupled-wave equations in a non-absorbing medium is presented. The solutions are derived beyond the SVA approximation up to order of κ/k (coupling constant over the wave number). The intensity distributions of the signal and the idler waves show a periodic behavior about their corresponding distributions of SVA-adapted solution. This behavior can be explained by the interference of the forward propagating signal (idler) wave and the corresponding backward one resulted from the reflection by the end face of the medium. Furthermore, this interference pattern in the medium can in turn serve as a periodic source for the next generations of the signal and idler waves. Therefore, the superposition of the waves, generated from different points of this periodic source, at the exit face of the medium shows an oscillatory behavior of the transmitted signal (idler) wave in terms of normalized coupling constant, κL. This study also shows that this effect is more considerable for high intensity pump beam, high relative refractive index and short length of the nonlinear medium.

Keywords. Nonlinear optics; frequency down convertor; parametric amplification.

PACS Nos 42.90.+m; 42.25.-p

1. Introduction

In OPA, two beams, namely, the pump beam and signal beam of frequencies $\nu_{\rm p}$ and $\nu_{\rm s}$ are incident on a nonlinear crystal. After mixing via the second-order polarization of the medium, a third beam with the difference frequency, $\nu_{\rm p}-\nu_{\rm s}$, called idler wave, $\nu_{\rm i}$, is generated. Under proper conditions the idler wave can mix with the pump wave to enhance the signal wave. This process continues, leading to an increase in power at $\nu_{\rm s}$ and $\nu_{\rm i}$ accompanied by a decrease in power for the pump beam ([1], §9.1, [2,3]).

Optical parametric amplification is increasingly used in photonics to generate wavelengths not available by conventional lasers [4]. Also the resonance configuration of this process, in which only the pump beam is present as the input, has been widely used in tunable lasers [5–7]. In this process a resonator consisting of the crystal provide a feedback at either the signal frequency or the idler one.

Nowadays, OPA has some applications in generating single- or two-mode squeezed states of light [8–10], as a source of entangled light beams and images [11,12] and in improving optical resolution [13].

Here, in this work, the coupled-wave equations of the non-degenerate parametric amplification is solved. This calculation has taken the second derivatives of the signal wave and its idler counterparts into account. These waves are normally distinguishable only by their polarization states. This is equivalent to considering a situation in which the forward propagating excited idler wave and amplified signal wave interfere with their corresponding backward reflected waves. Here, the effect of the backward waves is equivalent to keeping the second spatial derivatives of the fields in the coupled-wave equations, as was originally shown by Shen ([1], §3.3). The periodic behavior of the signal (idler) intensity distribution within the medium about the corresponding SVA distribution, resulted from the approach of this article, is an evidence of the occurrence of this interference. As a result of this interference, the signal and idler transmittances show an oscillatory behavior with respect to normalized coupling constant κL. In this article, a physical model describing this oscillatory behavior will be reported.

Similar approach has been already utilized by degenerate four-wave mixing (DFWM) phenomenon and an oscillatory dependence of both reflectance and transmittance in terms of the normalized coupling constant κL has been reported [14]. Here, we also observe the same behavior for the transmittance of the signal (idler) wave raising a different reason for its occurrence.

A brief review of OPA in SVA approximation is given in §2. The solution for coupled-wave equations of OPA beyond SVA approximation and its physical interpretation is given in §3, and finally the article will be discussed and concluded in §4 and 5.

2. Optical parametric amplification in SVA approximation

Optical parametric amplification simply is the transfer of energy from pump beam at $\omega_3(\omega_{\rm p})$ to the signal and idler beams at frequencies $\omega_1(\omega_{\rm s})$ and $\omega_2(\omega_{\rm i})$. Let us consider the situation in figure 1. Two optical waves at frequencies ω_3 and ω_1 with amplitudes A_3 and A_1 interact with each other in a lossless nonlinear medium, via the second-order susceptibility, to produce an output wave at frequency $\omega_2 = \omega_3 - \omega_1$ with amplitude A_2. The pump wave is usually assumed to be so strong, i.e. is undepleted by the nonlinear interactions.

In plane-wave approximation the equation for the pump, signal, and idler waves propagating along the z-axis with wave numbers k_3, k_1, and k_2 and amplitudes A_3, A_1, and A_2, respectively, can be written as [3]

$$E_3 = A_3(z)\exp[\imath(k_3 z - \omega_3 t)] + \text{c.c.}, \tag{1}$$

$$E_1 = A_1(z)\exp[\imath(k_1 z - \omega_1 t)] + \text{c.c.}, \tag{2}$$

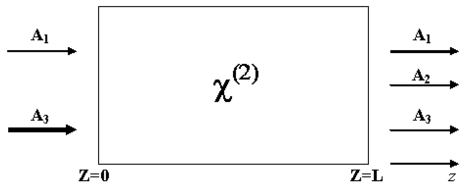

Figure 1. Schematic view of optical parametric amplification.

$$E_2 = A_2(z)\exp[\imath(k_2 z - \omega_2 t)] + \text{c.c.} \tag{3}$$

The corresponding second-order electric polarization equations, that control the generation of E_1 and E_2 are

$$P_1 = 2\chi^{(2)} A_3 A_2^* \exp[\imath(k_3 - k_2)z], \tag{4}$$

$$P_2 = 2\chi^{(2)} A_3 A_1^* \exp[\imath(k_3 - k_1)z], \tag{5}$$

where $\chi^{(2)}$ is the second-order nonlinear susceptibility. The wave equations for E_1 and E_2 are [3]

$$\frac{\mathrm{d}^2 E_i}{\mathrm{d}z^2} = \frac{\omega_\mathrm{i}^2}{c^2}\epsilon^{(1)}(\omega_\mathrm{i})E_i + \frac{4\pi\omega_\mathrm{i}^2}{c^2}P_i, \quad i = 1, 2. \tag{6}$$

In the SVA approximation, $\mathrm{d}^2 A_i/\mathrm{d}z^2 \ll k_i \mathrm{d}A_i/\mathrm{d}z$ for $i = 1, 2$. So eq. (6) reduces to [2,3]

$$\frac{\mathrm{d}A_1}{\mathrm{d}z} = \frac{4\pi\imath\omega_1^2\chi^{(2)}}{k_1 c^2} A_3 A_2^* \exp(\imath\Delta k z), \tag{7}$$

and

$$\frac{\mathrm{d}A_2}{\mathrm{d}z} = \frac{4\pi\imath\omega_2^2\chi^{(2)}}{k_2 c^2} A_3 A_1^* \exp(\imath\Delta k z), \tag{8}$$

where $\Delta k = k_3 - k_1 - k_2$. The coupled eqs (7) and (8) can be solved for A_1 and A_2 in terms of the boundary values of A_1 and A_2 at $z = 0$. In perfect phase matching condition and for $A_2(0) = 0$, the solutions are $[2, 3]$

$$A_1(z) = A_1(0)\cosh(\kappa z), \tag{9}$$

$$A_2(z) = \imath\left(\frac{n_1\omega_2}{n_2\omega_1}\right)^{1/2} \frac{A_3}{|A_3|} A_1^*(0)\sinh(\kappa z), \tag{10}$$

where $\kappa^2 = (16\pi^2(\chi^{(2)})^2\omega_1^2\omega_2^2/k_1 k_2 c^4)|A_3|^2$ is the coupling constant and n_1 and n_2 are refractive indices of the medium at signal and idler frequencies, respectively.

The nature of this SVA solution shows a continuous growth of the signal A_1 and the idler A_2. In the following section, eq. (6) is solved analytically up to order of κ/k without the SVA approximation for the case in which $\omega_1 = \omega_2 = \omega$ or $k_1 = k_2 = k$. Thus, in this situation the coupling constant becomes $\kappa^2 = 16\pi^2 k^2(\chi^{(2)})^2|A_3|^2$ and it will be shown that the behavior of the solution is different from that of the SVA approximation.

3. Optical parametric amplification beyond the SVA approximation

Keeping the second-order derivatives of A_1 and A_2 in eq. (6), the coupled-wave equations become

$$\frac{\mathrm{d}^2 A_1}{\mathrm{d}z^2} - 2\imath k_1 \frac{\mathrm{d}A_1}{\mathrm{d}z} = \frac{4\pi\omega_1^2\chi^{(2)}}{c^2} A_3 A_2^* \tag{11}$$

and

$$\frac{\mathrm{d}^2 A_2}{\mathrm{d}z^2} - 2\imath k_2 \frac{\mathrm{d}A_2}{\mathrm{d}z} = \frac{4\pi\omega_2^2\chi^{(2)}}{c^2} A_3 A_1^*. \tag{12}$$

If simultaneous solutions of eqs (11) and (12) is desired for the case $\omega_1 = \omega_2$, one would lead to the following equation for $A_1(z)$:

$$\frac{\mathrm{d}^4 A_1}{\mathrm{d}z^4} + 4k^2 \frac{\mathrm{d}^2 A_1}{\mathrm{d}z^2} - 4\kappa^2 k^2 A_1 = 0, \tag{13}$$

where $A_1(z)$ and $A_2(z)$ are just distinguished by their polarization states. The general solution of eq. (13) up to order of κ/k can be written as

$$A_1(z) = C_1 \exp(\kappa z) + C_2 \exp(-\kappa z) + C_3 \exp(2\imath kz) + C_4 \exp(-2\imath kz). \tag{14}$$

The first two terms of eq. (14) are similar to the SVA solution but the last two terms are new and imply an oscillation with spatial frequency $2k$. To determine the constants in eq. (14), suitable boundary conditions should be applied. These conditions are

$$A_2(0) = 0 \tag{15}$$

and

$$A_1(0^+) = A_1(0^-), \tag{16}$$

where + or − indicate moving to the boundaries from right or left, respectively. Continuity of the tangential components of electric fields at $z = L$ for signal and idler amplitudes gives

$$A_2(L^-) \exp(-\imath kL) = A_2(L^+) \exp(-\imath k_\mathrm{o} L) \tag{17}$$

and

$$A_1(L^-) \exp(-\imath kL) = A_1(L^+) \exp(-\imath k_\mathrm{o} L), \tag{18}$$

where k and k_o show the wavelengths inside and outside the medium, respectively. Also, the continuity of tangential components of magnetic fields at $z = L$ leads to

$$\exp(-\imath kL) \frac{\mathrm{d}A_2}{\mathrm{d}z}\Big|_{L^-} - \imath k A_2(L^-) \exp(-\imath kL) = -\imath k_\mathrm{o} A_2(L^+) \exp(-\imath k_\mathrm{o} L) \tag{19}$$

and

$$\exp(-\imath kL)\frac{\mathrm{d}A_1}{\mathrm{d}z}\mid_{L^-} -\imath kA_1(L^-)\exp(-\imath kL) = -\imath k_{\mathrm{o}}A_1(L^+)\exp(-\imath k_{\mathrm{o}}L). \tag{20}$$

Using these boundary conditions and keeping only the terms up to order of κ/k and after a series of long calculations, the solution for $A_1(z)$, eq. (14), can be written as

$$A_1(z) = \Big[\frac{a_1}{b}\exp(\kappa z) + \frac{a_2}{b}\exp(-\kappa z) + \frac{a_3}{b'}\exp(2\imath kz) + \frac{a_4}{b'}\exp(-2\imath kz)\Big] A_1(0), \tag{21}$$

where a_1, a_2, a_3, a_4, b, and b' are

$$a_1 = 2(n+1)[(n+1)\exp(\kappa L) + (n-1)\exp(2\imath kL)], \tag{22}$$

$$a_2 = 2\exp(\kappa L)(n+1)[1+n+(n-1)\exp(\kappa+2\imath k)L], \tag{23}$$

$$a_3 = -\imath 8\exp(\kappa L)(n-1)^2 + \Bigg[-4\imath(1+\exp(2\kappa L))(n^2-1) + (\exp(2\kappa L)-1)(1+7n^2)\frac{\kappa}{k}\Bigg]\exp(-2\imath kL), \tag{24}$$

$$a_4 = (\exp(2\kappa L)-1)(n^2-1)\frac{\kappa}{k}\exp(2\imath kL), \tag{25}$$

$$b = 8\exp(\kappa L)(1+n^2) + 4\Bigg[(1+\exp(2\kappa L))(n^2-1) + \imath(\exp(2\kappa L)-1)n^2\frac{\kappa}{k}\Bigg]\cos 2kL + (\exp(2\kappa L)-1)(1+3n^2)\frac{\kappa}{k}\sin 2kL, \tag{26}$$

$$b' = 8\left[-\imath(1+\exp(2\kappa L))(n^2-1) + (\exp(2\kappa L)-1)n^2\frac{\kappa}{k}\right]\cos 2kL - 2\imath\left[8\exp(\kappa L)(1+n^2) + (\exp(2\kappa L)-1)(1+3n^2)\frac{\kappa}{k}\sin 2kL\right]. \tag{27}$$

In eqs (22)–(27), n is the relative refractive index. From eqs (11) and (14), one obtains $A_2(z)$, for the amplitude of the idler wave in the medium as

$$A_2(z) = \frac{1}{2k\kappa}\left[\frac{a_1^*}{b^*}(\kappa^2 - 2\imath k\kappa)\exp(\kappa z) + \frac{a_2^*}{b^*}(\kappa^2 + 2\imath k\kappa)\exp(-\kappa z) - 8k^2\frac{a_4^*}{b'^*}\exp(-2\imath kz)\right]A_1(0), \qquad (28)$$

where $*$ indicates the complex conjugate.

To elucidate the behavior of the signal and the idler waves, namely, eqs (21) and (28) respectively, we obtain the intensity distribution of these waves in the medium and their corresponding transmittances. Using eq. (21) the normalized intensity of the signal wave can be written as

$$\begin{aligned}\frac{|A_1(z)|^2}{|A_1(0)|^2} &= \frac{a_1a_2^* + a_2a_1^*}{|b|^2} + \frac{|a_3|^2 + |a_4|^2}{|b'|^2} + \frac{|a_1|^2}{|b|^2}\exp(2\kappa z) \\ &+ \frac{|a_2|^2}{|b|^2}\exp(-2\kappa z) + \left[\frac{a_1a_3^*}{bb'^*}\exp(\kappa - 2\imath k)z + \text{c.c.}\right] \\ &+ \left[\frac{a_1a_4^*}{bb'^*}\exp(\kappa + 2\imath k)z + \text{c.c.}\right] + \left[\frac{a_2a_3^*}{bb'^*}\exp -(\kappa + 2\imath k)z + \text{c.c.}\right] \\ &+ \left[\frac{a_2a_4^*}{bb'^*}\exp(-\kappa + 2\imath k)z + \text{c.c.}\right] + \left[\frac{a_3a_4^*}{|b'|^2}\exp 4\imath kz + \text{c.c.}\right]. \qquad (29)\end{aligned}$$

Also, by using eq. (28) the normalized intensity of the idler wave is given by

$$\begin{aligned}\frac{|A_2(z)|^2}{|A_1(0)|^2} &= \frac{|a_1|^2}{|b|^2}\exp(2\kappa z) + \frac{|a_2|^2}{|b|^2}\exp(-2\kappa z) + 16\frac{k^2}{\kappa^2}\frac{|a_4|^2}{|b'|^2} \\ &+ \left[\frac{a_1^*a_2}{|b|^2}\left(-1 - \imath\frac{\kappa}{k}\right) + \text{c.c.}\right] \\ &+ \left[\frac{a_1^*a_4}{b^*b'}\left(4\imath\frac{k}{\kappa} - 2\right)\exp(\kappa + 2\imath k)z + \text{c.c.}\right] \\ &- \left[\frac{a_2^*a_4}{b^*b'}\left(4\imath\frac{k}{\kappa} + 2\right)\exp(-\kappa + 2\imath k)z + \text{c.c.}\right]. \qquad (30)\end{aligned}$$

If we insert $z = L$ in eqs (29) and (30), we obtain the transmittances for the signal and the idler waves, respectively.

4. Discussion

In order to understand the physical meaning of this approach we investigate the spatial dependence of the signal and the idler intensities in the medium. According to eqs (29) and (30) one can describe the intensity variations of the waves along the medium for different values of n and κ/k. This is shown in figure 2 for $n = 1.9$ and $\kappa/k = 0.1/10 = 0.01$, the signal and the idler intensity distributions have an oscillatory behavior in the neighborhood of their corresponding SVA smooth curves. The amplified signal wave (upper curve) and the generated idler wave

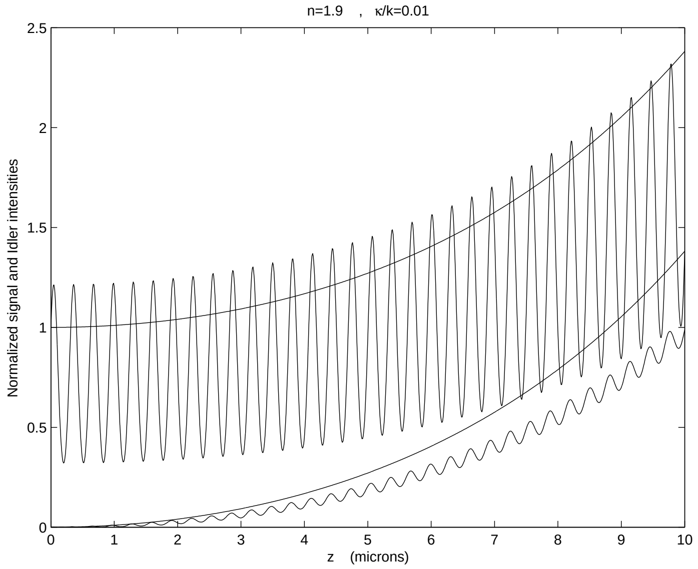

Figure 2. Periodic variation of the normalized signal (upper curve) and idler (lower curve) intensities with respect to z, for $n = 1.9$ and $\kappa/k = 0.01$. The smooth curves indicate the corresponding SVA solutions.

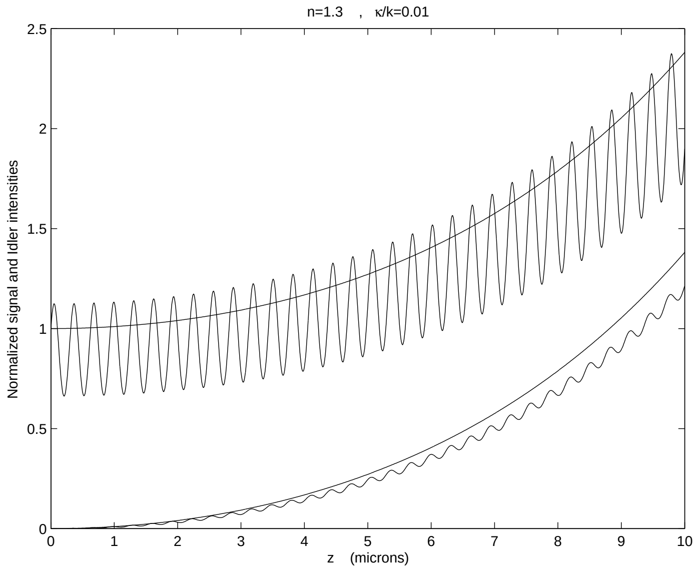

Figure 3. Variation of the normalized signal (upper curve) and idler (lower curve) intensities with respect to z, for $n = 1.3$ and $\kappa/k = 0.01$. The amplitude of oscillation in both intensity distributions becomes smaller compared to the one for $n = 1.9$. The smooth curves indicate the corresponding SVA solutions.

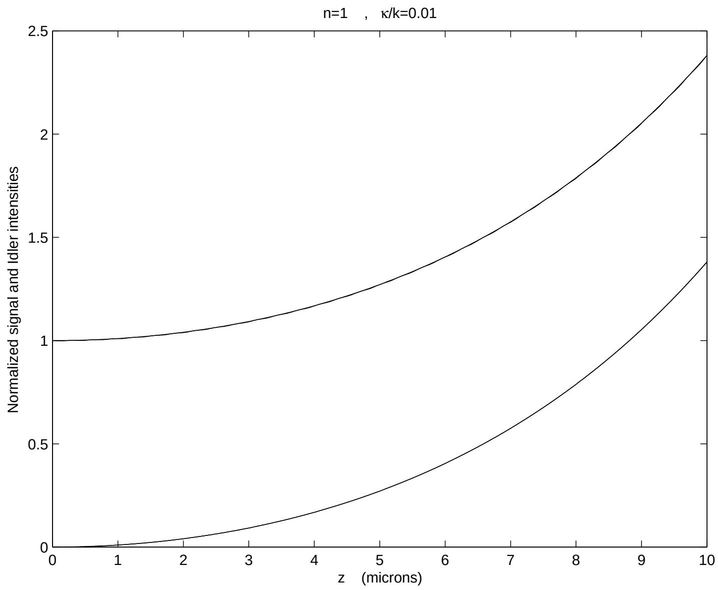

Figure 4. Variation of the signal intensity (upper curve) and idler intensity (lower curve) with respect to z, for $n = 1.0$ and $\kappa/k = 0.01$. The amplitude of oscillation becomes very small and our solutions reduce to the corresponding one in SVA approximation.

(lower curve) have the same oscillatory feature, but their amplitudes are different. The occurrence of this oscillatory behavior can be explained as follows. Beyond the SVA approximation for the solution of the fourth-order equation, eq. (13), we need to consider extra boundary conditions at the end face of the medium. Applying these boundary conditions is analogous to considering the reflection and transmission of the signal (idler) wave at the end face, $z = L$ (see figure 1). The oscillatory behavior could be due to the interference between the forward signal (idler) wave and the corresponding backward reflected wave. In figures 3 and 4 the normalized signal and idler intensities vs. z are plotted for $n = 1.3$ and 1, respectively. Comparing these graphs with the graph in figure 2, we notice that the oscillatory behavior strongly depends on relative refractive index (n) and decreases as n decreases. On the other hand, by increasing the relative refractive index, the reflectance at the end face increases and this enhances the signal and idler waves and consequently increases the oscillation amplitude which is due to the interference phenomena. Figure 4 shows $n = 1$ case where no oscillation is seen since there is no reflection (no backward signal (idler) wave) from the end face and therefore our solutions reduce to the corresponding ones in SVA approximation. Figures 5 and 6 show the amplitude of oscillation of signal and idler intensity distributions for larger length of the crystal. The amplitude of oscillation does not however remain uniform everywhere and becomes larger near the end of the medium. In fact, this feature can also be deduced from figures 2 and 3 for the case of the shorter length of the crystal.

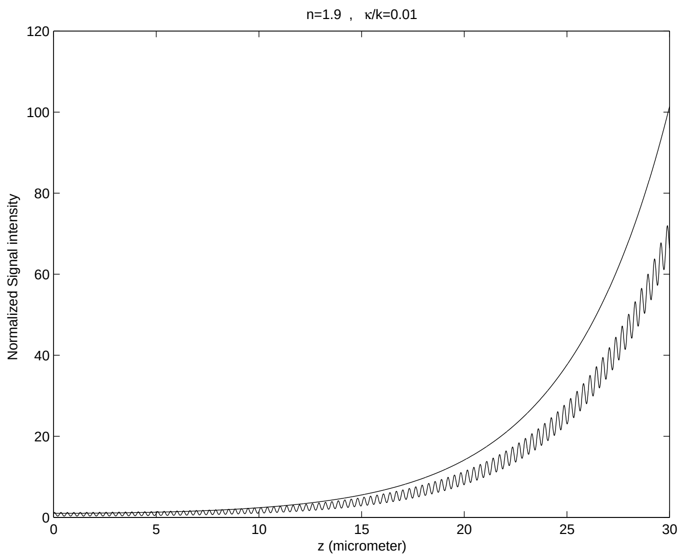

Figure 5. Variation of the signal intensity (lower curve) with respect to z, for $n = 1.9$ and $\kappa/k = 0.01$. The amplitude of oscillation decreases when the length of (z) increases from 10 to 30 microns. The upper smooth curve represents the corresponding SVA solution.

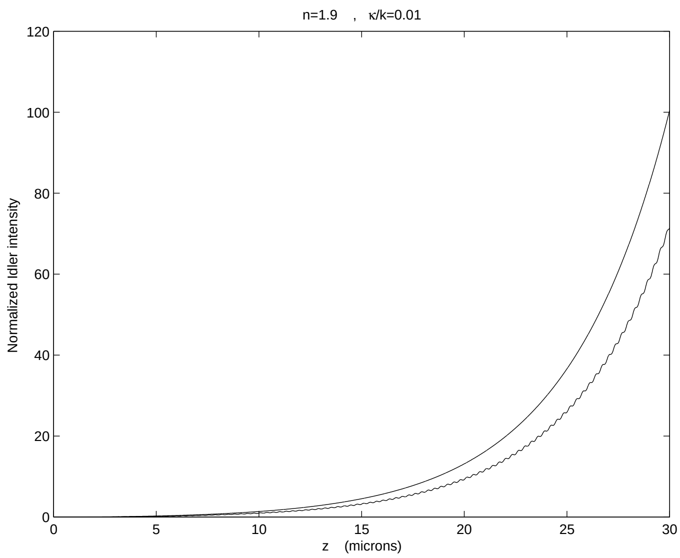

Figure 6. Variation of the idler intensity (lower curve) with respect to z, for $n = 1.9$ and $\kappa/k = 0.01$. The amplitude of oscillation decreases when the length of the medium (z) increases from 10 to 30 microns. The upper smooth curve represents the corresponding SVA solution.

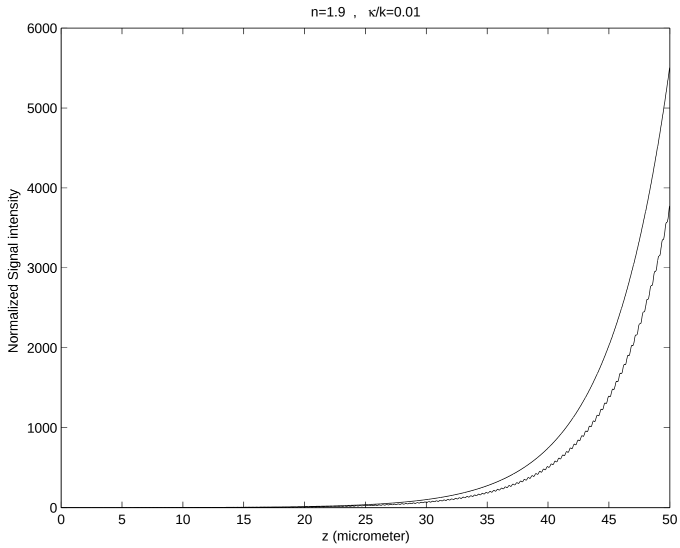

Figure 7. Variation of the signal intensity (lower curve) with respect to z, for $n = 1.9$ and $\kappa/k = 0.01$. When the length is increased from 30 to 50 microns, the amplitude of oscillation becomes very small and our solution nearly reduces to the corresponding one in SVA approximation (upper curve).

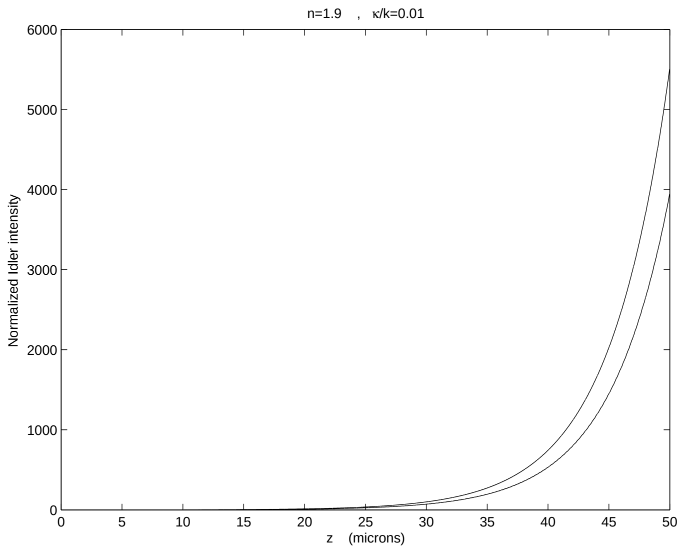

Figure 8. Variation of the idler intensity (lower curve) with respect to z, for $n = 1.9$ and $\kappa/k = 0.01$. When the length is increased from 30 to 50 microns, the amplitude of oscillation becomes very small and our solution behaves like the corresponding one in SVA approximation (upper curve).

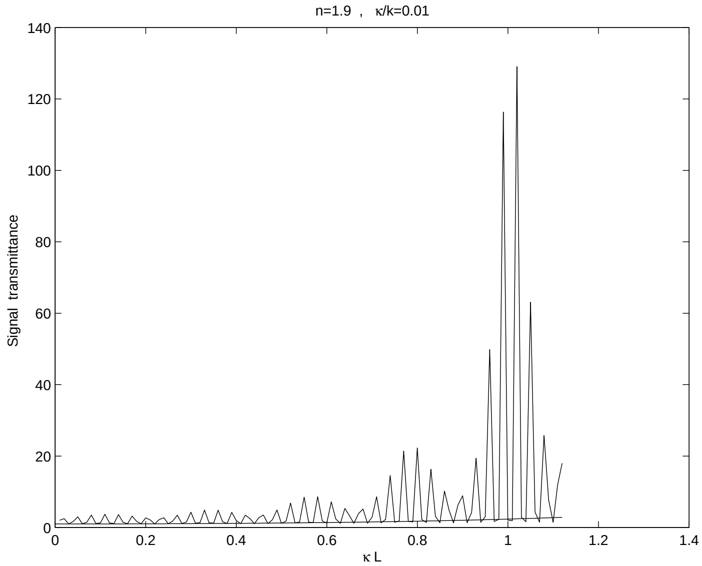

Figure 9. Signal transmittance with respect to κL, for $n = 1.9$ and $\kappa/k = 0.01$. The transmittance have an oscillatory behavior around the transmittance in SVA approximation (smooth curve).

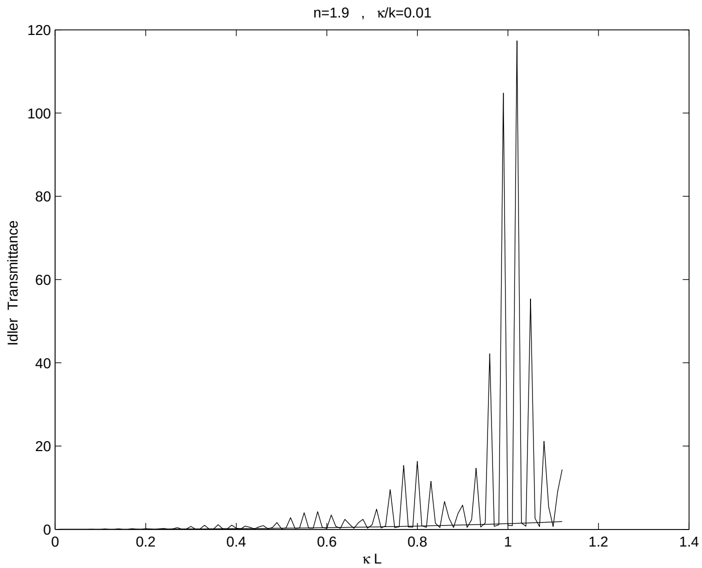

Figure 10. Idler transmittance with respect to κL, for $n = 1.9$ and $\kappa/k = 0.01$. Similar to figure 5 the transmittance have an oscillatory behavior around the corresponding one in SVA approximation.

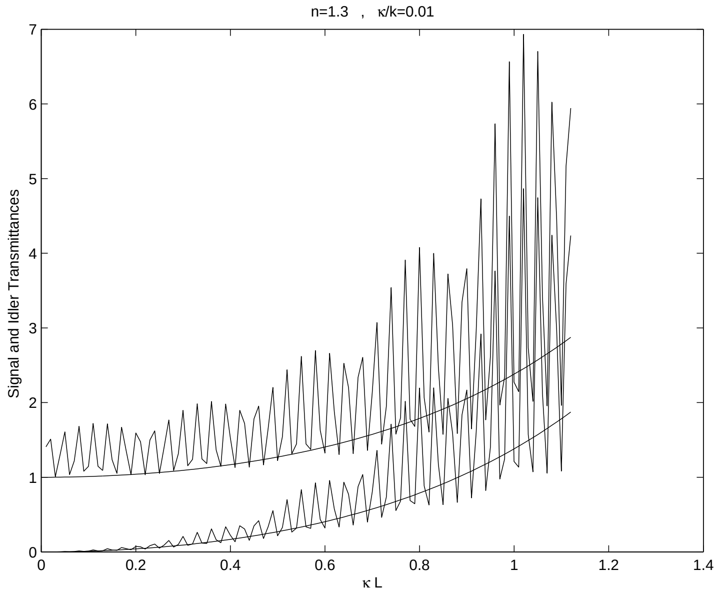

Figure 11. Variation of the signal (upper curve) and idler (lower curve) transmittances with respect to κL, for $n = 1.3$ and $\kappa/k = 0.01$. The amplitude of oscillation becomes smaller compared to the one for $n = 1.9$.

On the other hand, when the relative refractive index of the medium is constant the oscillations accompanied by the growing intensity are more appreciable for short length medium than that of long length medium (see figures 5–8 and compare to figure 2).

Now, one can describe the intensity variation of the signal and idler waves (with linear polarizations orthogonal to each other) in the medium and its effect on the signal and idler transmittances. The graphs in figures 9 and 10 show the oscillatory behavior of the signal and idler transmittances for $n = 1.9$ and $\kappa/k = 0.01$ respectively, as a function of the normalized coupling constant, κL. The physical interpretation of this behavior can be explained in a process as follows. It is known that in OPA the transmitted signal (or idler) wave at $z = L$ results from the coherent superposition of all signal (or idler) waves originated at different regions of the medium before $z = L$. Here, due to interference between the forward and the backward signal (or idler) waves, the contribution of different regions of the medium in the generation of the signal (or idler) wave at $z = L$ obeys a periodic distribution. Under these circumstances and due to the relative phase differences of the signal (or idler) waves arriving at the end of medium ($z = L$), constructive or destructive interference occurs, and consequently the fast oscillations would be seen in signal (or idler) transmittance (figures 9–11). Furthermore, the fast oscillating signal (or idler) can also be reflected from the end face of the medium. Hence, reflected backward (fast oscillating) signal (or idler) may be interfered with the corresponding one in the forward direction and produce other oscillations in the

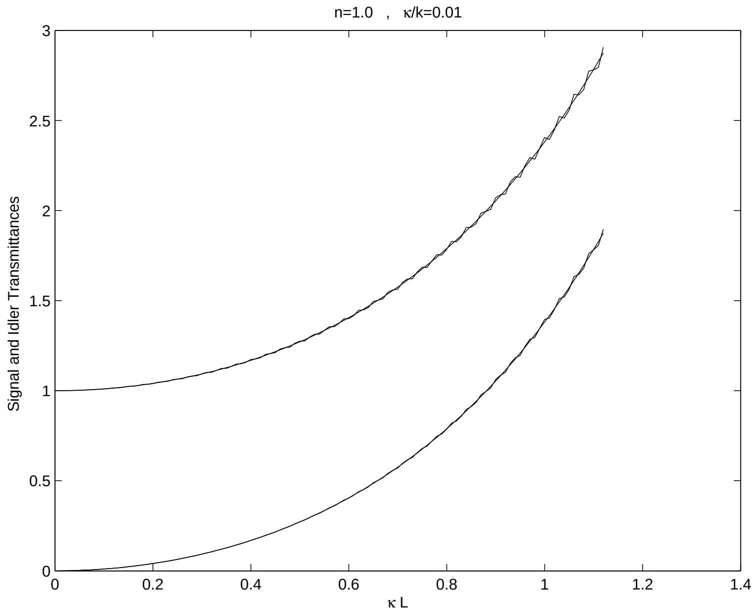

Figure 12. Variation of the signal (upper curve) and idler (lower curve) transmittances with respect to κL, for $n = 1.0$ and $\kappa/k = 0.01$. The amplitude of oscillation around the corresponding curves in SVA approximation (smooth curves) becomes very small.

signal (or idler) transmittance. Slow oscillations modulated on the fast ones in the signal (or idler) transmittance is the result of this interference (figures 9–11). By comparing figure 11, for $n = 1.3$ and $\kappa/k = 0.01$, with figure 12, for $n = 1$ and $\kappa/k = 0.01$, one can see that the oscillations in signal (idler) transmittance decrease when the relative index of refraction approaches unity. Figure 13 shows that when $n = 1$ and $\kappa/k = 0.01/100 = 0.0001$ (pump intensity is lower compared to figure 12), the signal (idler) transmittance completely coincides with the corresponding one in the SVA solution. Since for $n = 1$, there is no difference between the non-linear medium and its surrounding, the end boundary surface of the medium is non-existent. Therefore, the oscillatory features in the intensity distributions and in the transmittances, resulting from the reflection at the end boundary surface, disappear and the solutions reduce to the corresponding ones in SVA solution, as can be seen from figures 4 and 13.

Therefore, according to the above discussion 'the OPA beyond SVA approximation', when the signal and idler waves are distinguished only by their orthogonal polarizations, is more appreciable for media of short lengths (less than 50 micrometer for $\lambda = 500$ nm) and high relative refractive indices. Besides, one must apply high pump intensity in a medium with high second-order susceptibility ($\chi^{(2)}$) in order to adjust the value of κ/k.

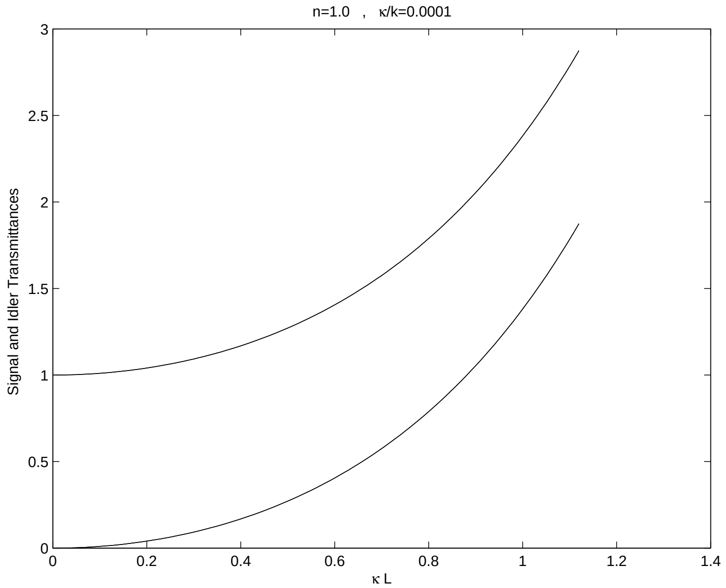

Figure 13. Variation of the signal and idler transmittances, the upper and the lower curves respectively, with respect to κL, for $n = 1$ and $\kappa/k = 0.0001$. The amplitude of oscillation vanishes and the graphs belong to our solution and the corresponding one in SVA approximation completely cover each other.

5. Conclusion

The coupled-amplitude equations of the optical parametric amplification are solved analytically beyond the SVA approximation up to order of κ/k for the non-resonant interactions, where the signal and the idler waves have the same frequency but distinguishable by their polarizations. In this approach all waves are considered to be plane waves and pump wave is undepleted. Taking into account the second-order derivatives of the signal and idler waves in the coupled wave equations is equivalent to considering the effect of the end face of the medium on the propagation of these waves. The solution indicates that the intensity distribution of the signal and idler waves in the medium has a periodic variation near the corresponding distributions in SVA approximation solution. This leads to an oscillatory dependence of the signal (idler) transmittance on the normalized coupling constant and the amplitude of this oscillation significantly changes with relative refractive index of the medium. This behavior can be explained in a process which is begun by considering the effect of the interference between the forward propagating signal (idler) wave and the corresponding backward propagating wave resulting from reflection at the end face of the medium. After this interference, the medium behaves like a periodic distributed source of the signal (idler) wave which in turn produces more signal (idler) wave. Therefore, in this stage, the phase difference between signal waves originating at different parts of the medium cause constructive or destructive patterns as they arrive at the end face of the medium. This effect can be seen as the fast oscillations in signal (idler) transmittance. The amplitude of oscillations in the signal and idler transmittances strongly depend on the relative refractive index of the medium. When relative refractive index is unity ($n = 1$), there is no difference between the nonlinear medium and its surrounding, in fact the end boundary surface of the medium is non-existent. Since there is no reflection from the end boundary surface of the medium, the oscillatory behavior in the signal (idler) intensity distribution and its transmittance disappear and the solution reduces to the corresponding one in SVA solution.

It is recommended that for observing the oscillatory behavior in signal and idler transmittances when they differ from each other only by their linear polarization states (orthogonal to each other), the OPA must be performed in a medium with high relative refractive index and short length (less than fifty micrometer for $\lambda =$ 500 nm), see figures 2 and 5–8. Furthermore, one can adjust the desired value for κ/k by employing the high pump intensity in a medium with high $\chi^{(2)}$ value.

This work has been continued toward the quantum treatment of this approach to study the squeezing property of the output mode.

Acknowledgment

The author thanks M T Tavassoly of Tehran University and Institute for Advanced Studies in Basic Sciences, Zanjan, Iran, for helpful comments and discussions. The author also gratefully acknowledges H Nadgran of Physics Department, Shiraz University for helpful comments.

References

[1] Y R Shen, *The principles of nonlinear optics* (John-Wiley and Sons, Hoboken, New Jersey, 1984), Wiley Classics Library Edition, published 2003. ISBN: 0-471-43080-3
[2] R W Boyd, *Nonlinear optics* (Academic Press, 1991) chap. 2
[3] Special issue on optical parametric oscillation and amplification, *J. Opt. Soc. Am.* **B10**, 1659 (1993)
[4] J H Hunt, *Optical parametric oscillators and amplifiers and their applications* (SPIE Optical Engineering Press, London, 1997)
[5] M H Dunn and M Ebrahimzadeh, *Science* **286**, 1513 (1999)
[6] W Koechner, *Solid-state laser engineering*, 5th ed. *Springer series in optical sciences*, chap. 10, sec. 2 (1999)
[7] M B Radunsky, *Laser Focus World* **31**, 107 (1995)
[8] J Anwar and M S Zubairy, *Phys. Rev.* **A45**, 1804 (1992)
[9] Marlan O Scully and M Suhail Zubairy, *Quantum optics* (Cambridge, 2001), chap. 16
[10] R Loudon, *The quantum theory of light*, third ed., (Oxford University Press, 2000) chap. 9
[11] Elna M Nagasako, Sean Bentley, R W Boyd and G S Agarwal, *Phys. Rev.* **A64**, 043802 (2001)
[12] A Gatti, E Brambilla, L A Lugiato and M I Kolobov, *Phys. Rev. Lett.* **83(9)**, 1763 (1999)
[13] M I Kolobov and C Fabre, *Phys. Rev. Lett.* **85(18)**, 3789 (2000)
[14] M Hosseini Farzad and M T Tavassoly, *J. Opt. Soc. Am.* **B14(7)**, 1707 (1997)